Separation Science and Technology
Publication details, including instructions for authors and subscription information:
http://www.informaworld.com/smpp/title~content=t713708471

Chromate Removal from Water Using Surfactant-Enhanced Crossflow Filtration

B. Keskinler[a]; U. Danis[a]; A. Çakici[b]; G. Akay[c]
[a] DEPARTMENT OF ENVIRONMENTAL ENGINEERING, ATATÜRK UNIVERSITY, ERZURUM, TURKEY [b] DEPARTMENT OF CHEMICAL ENGINEERING, ATATÜRK UNIVERSITY, ERZURUM, TURKEY [c] DEPARTMENT OF CHEMICAL ENGINEERING, UNIVERSITY OF NOTTINGHAM, NOTTINGHAM, UK

To cite this Article Keskinler, B. , Danis, U. , Çakici, A. and Akay, G.(1997) 'Chromate Removal from Water Using Surfactant-Enhanced Crossflow Filtration', Separation Science and Technology, 32: 11, 1899 — 1920
To link to this Article: DOI: 10.1080/01496399708000744
URL: http://dx.doi.org/10.1080/01496399708000744

SEPARATION SCIENCE AND TECHNOLOGY, 32(11), pp. 1899–1920, 1997

Chromate Removal from Water Using Surfactant-Enhanced Crossflow Filtration

B. KESKINLER and U. DANIS
DEPARTMENT OF ENVIRONMENTAL ENGINEERING
ATATÜRK UNIVERSITY
25240 ERZURUM, TURKEY

A. ÇAKICI
DEPARTMENT OF CHEMICAL ENGINEERING
ATATÜRK UNIVERSITY
25240 ERZURUM, TURKEY

G. AKAY*
DEPARTMENT OF CHEMICAL ENGINEERING
UNIVERSITY OF NOTTINGHAM
NOTTINGHAM, NG7 2RD, UK

ABSTRACT

Removal of chromate from water was investigated using the surfactant enhanced crossflow filtration technique in which the cationic surfactant, cetyl trimethylammonium bromide (CTAB), was the carrier for the metal ions. The variation of chromate and surfactant rejections, and permeate flux with time were measured as a function of CTAB/chromate concentration ratio, while maintaining a constant transmembrane pressure drop, membrane pore size, and pH of the feed solution. The method was found to be effective in removing chromate from water. It was observed that the efficiency of chromate removal increased with increasing CTAB/chromate ratio. It was also found that the chromate concentration had a significant effect on the CTAB concentration in the permeate and on the time taken to establish the secondary membrane which consists of a highly viscous surfactant phase in the hexagonal state in the absence of chromate. In the presence of chromate, permeate flux increased at the same CTAB concentration although the surfactant and chromate rejections decreased, indicating lowering of the secondary membrane resistance to permeate flow. These conclusions were confirmed by dead-

* To whom correspondence should be addressed.

end filtration experiments which showed that the fouling index decreased by the addition of chromate while the opposite was valid when sodium chloride was present in the surfactant/water/electrolyte ternary system.

Key Words. Crossflow filtration; Surfactant enhanced filtration; Chromate removal; Wastewater treatment; Surfactant removal

INTRODUCTION

Crossflow ultrafiltration is an effective low energy separation process for macromolecules or supermolecular systems such as lyotropic liquid crystals formed by surfactants in aqueous media. Both water-soluble polymers and surfactants are used as effective carriers for the removal of heavy metal ions or organic pollutants from water using the so-called micellar-enhanced ultrafiltration (MEUF) technique (1–5).

The removal of surfactants (in the absence or presence of electrolyte/heavy metal ions) from water using crossflow filtration has been studied extensively during the 1970s, notably by Bhattacharyya (see, for example, ref. 7 for a review of the subject). More recently, such studies were extended to establish the mechanism of crossflow filtration of surfactants, polymeric surfactants, and other self-associating solute systems (8–13). The enhancement of permeate flux and surfactant rejection by several orders of magnitude has been achieved in these systems using crossflow electrofiltration (14, 15). It has been shown in these studies that, under steady—state conditions, the surfactant rejection and permeate flux are primarily controlled by the secondary membrane formed by the deposition of the surfactant on the primary membrane surface and within the pores. The surfactant in the secondary membrane is in a highly viscous phase (such as lamellar or hexagonal state) which could be predicted from the phase diagram of the surfactant (8, 9).

The surfactant concentration and membrane pore size ranges can be extended over and above those employed in MEUF when surfactants are used as carriers for heavy metal ions (16–18). In this case also, both the surfactant and ion rejections and permeate flux are also controlled by the secondary membrane. However, due to the binding of the electrolyte to the surfactant, physicochemical characteristics of the secondary membrane are modified, which subsequently alters its filtration behavior.

Under steady-state conditions the concentration of the surfactant on the primary membrane and within the pores (i.e., secondary membrane) can be predicted from the phase diagram of the surfactant/water binary system (8–10). It was found that the surfactant in the secondary membrane

was in a viscous phase such as lamellar, cubic, or hexagonal liquid crystalline state. Therefore, the lower estimate of the surfactant concentration in the secondary membrane can be readily obtained from the phase diagrams. Such phase diagrams are available for some surfactant/water binary systems as a function of temperature. However, there are no phase diagrams available for the surfactant/water/electrolyte ternary systems involving heavy metal ions. It is therefore not possible to give an estimate of the surfactant concentration in the secondary membrane when high valency electrolytes are present in the surfactant dispersion medium.

In order to circumvent the lack of data, we examined the effect of electrolyte on the secondary membrane structure through dead-end filtration experiments in which the specific cake resistance was measured. The specific cake resistance, α, is often used to characterize the hydrodynamic resistance of the secondary membrane (cake) during the filtration of particulate suspensions which, unlike the surfactant dispersions/solutions, do not undergo any phase change as a result of increased concentration upon deposition on the membrane. To a first-order approximation, particle concentration on the membrane may be taken as the random packing fraction of the particles although both the permeate flux and particle size distribution will create a concentration distribution across the cake. It can be shown that (19) the specific cake resistance in filtration is given by

$$\frac{t}{V} = R_m + \frac{\mu\alpha C_{SF}}{2\Delta P}V \tag{1}$$

where t is the filtration time, V is the volume of the permeate per unit filtration area, R_m is the primary membrane resistance, μ is the permeate viscosity which may be taken as the viscosity of water, ΔP is the transmembrane pressure, and C_{SF} is the feed surfactant concentration. Therefore, a plot of t/V vs V should give a straight line from the slope of which the modified fouling index (MFI) (19) can be calculated as

$$\text{MFI} = \frac{\mu\alpha C_{SF}}{2\Delta P} \tag{2}$$

In our previous study the removal of nitrate ions using surfactant enhanced crossflow filtration was reported (17, 18). In this study we consider the removal of chromium ions from water using the same technique. Chromium is usually found in the forms of chromate ions (CrO_4^{2-}) or dichromate ions ($Cr_2O_4^{2-}$), depending on the pH. However, chromate ions exist as stable anionic species over a wide pH range. Removal of chromate (or indeed other heavy metal ions) from water can also be achieved using reverse osmosis, electrodialysis, or electrodeposition techniques which require high operating pressures and/or consume large amounts of energy.

Therefore, the current technique, like MEUF (1), may be considered as an energy-efficient separation technique, especially if the high surfactant concentration levels could be tolerated. However, the purpose of this study is to understand the mechanism of crossflow filtration when surfactants are used as carriers for the removal of heavy metal ions. CTAB was chosen since its phase behavior is well known.

EXPERIMENTAL

Materials

Potassium chromate, sodium chloride (Merck, certified analytical grades), and cationic surfactant cetyl trimethylammonium bromide (hexadecyltrimethylammonium bromide) (CTAB) (Fluka, certified analytical grade) were used as received. The critical micellar concentration (CMC) of CTAB may be assumed to be 0.9 mM at 30°C. Distilled and deionized water was used for the preparation of all the solutions. The membrane (Schleicher and Schuell) was an anisotropic cellulose acetate membrane with a 0.2 μm pore size rating.

Dead-End Filtration Apparatus

The dead-end filtration apparatus shown in Fig. 1 had an effective surface area of 45.3 cm^2. The feed (20 L) was pumped through the filtration module at a predetermined transmembrane pressure drop, $\Delta P = 150$ kPa, at 30°C. The permeate rate was measured with an electronic balance, and data were stored as a function of time.

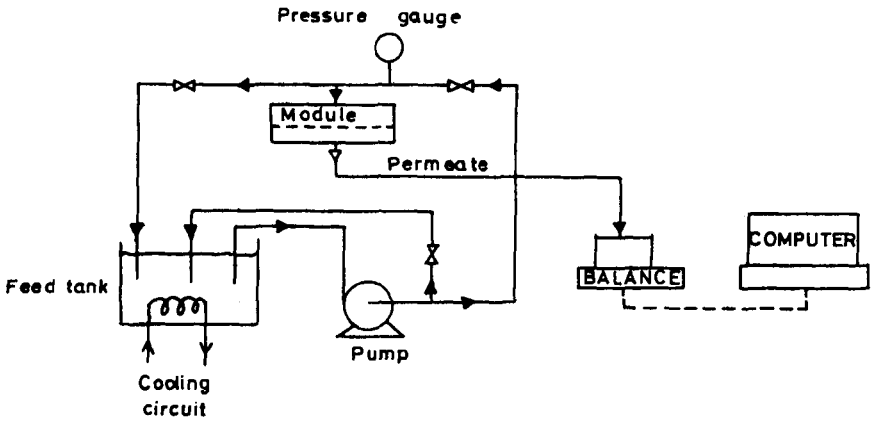

FIG. 1 Schematic diagram of the dead-end filtration apparatus.

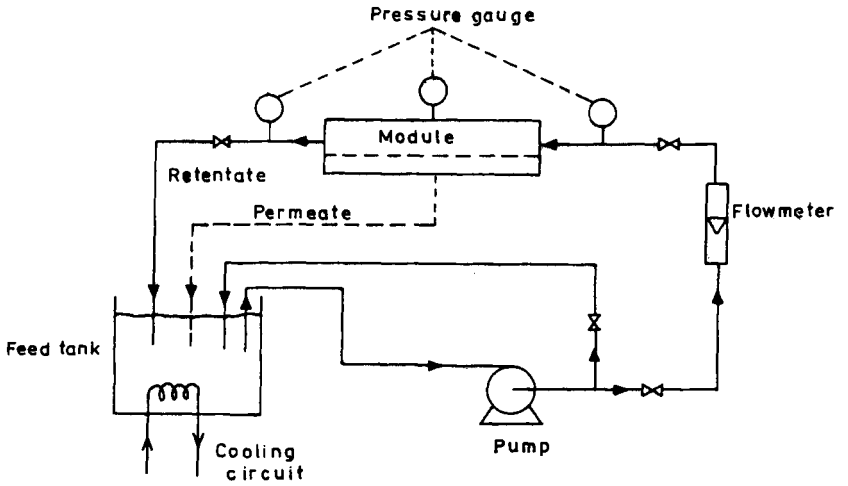

FIG. 2 Schematic diagram of the crossflow filtration apparatus.

Crossflow Filtration Apparatus

The experimental apparatus shown in Fig. 2 consisted of a flow circuit in which 20 L of distilled water containing a known amount of surfactant and chromate ions (feed solution) was pumped continuously through a crossflow filtration cell at a predetermined crossflow velocity (6 m/s) and transmembrane pressure drop (ΔP = 150 kPa). The desired filtration conditions were maintained by two manually operated valves. The temperature of the process solution was kept constant at 30°C by using a plate-type heat exchanger placed in the feed tank which has its own cooling circuit.

The purpose built filtration equipment consisted of a filtration cell which was constructed from plastic and stainless steel. Flat sheet membranes of 28 cm^2 effective surface area were placed into the cell to form a one-sided rectangular filtration channel of length 70 mm, width 40 mm, and 1.5 mm thickness. The filtrate produced was returned to the feed tank so that the feed surfactant concentration remained constant.

The feed solution was prepared at 30°C in the feed tank containing 20 L distilled water while recirculating through the by-pass line with the filter line shut. The desired amount of concentration in the process solution was obtained by adding a certain amount of active surfactant slowly into the feed tank. At the end of a 60-minute recirculation period a certain amount of chromate was slowly added into the feed tank in order to obtain the desired chromate concentration in the process solution. The recircula-

tion was continued for another 60 minutes prior to the start of the filtration process. During filtration, permeate decay was recorded. Permeate and feed conductivities were monitored, which indicated that during filtration there were no significant variations in pH (pH 7.25) or in the conductivities of the feed solution and permeate. The permeate samples were collected at predetermined time intervals and later analyzed for their surfactant and chromate concentrations. The permeate flux was determined gravimetrically.

Surfactant and Chromate Concentration Determination

Chromate concentrations were determined with a UV-Visible spectrophotometer (Shimadzu UV160A) at 540 nm wavelength. Surfactant concentration was determined by an Organic Carbon Analyser (Beckman 915A) with UNICAM 4815 computing integrator.

Calculation of the Chromate and Surfactant Rejections

The efficiency of the ultrafiltration process is defined by the conventional rejection coefficients, R_S and R_C, for CTAB and chromate rejections, respectively.

For the surfactant rejection:

$$R_S(t) = 1 - \frac{C_S(t)}{C_{SF}} \tag{3}$$

where $C_S(t)$ and C_{SF} are the surfactant concentrations in the permeate and feed streams, respectively, and for the chromate rejection:

$$R_C(t) = 1 - \frac{C_C(t)}{C_{CF}} \tag{4}$$

where $C_C(t)$ and C_{CF} are the chromate concentrations in the permeate and feed streams, respectively. C_S and C_C as well as R_S and R_C represent transient values and therefore they are time-dependent.

Ideally and for practical and theoretical purposes, permeate CTAB and chromate concentrations, and hence the rejections as well as the permeate flux under steady-state conditions, should also be determined experimentally. However, the establishment of the steady state may take an excessively long time. Therefore, we assume that "steady state" is established when, after an initial rapid decay, the decrease in flux appears to be very slow. In the present experiments this is usually achieved after 120 minutes of crossflow filtration. Within the limitations of the definition of steady state given above, the steady-state concentrations and rejections corre-

sponding to C_S, C_C, R_S, and R_C are denoted by C_S^*, C_C^*, R_S^*, and R_C^*, respectively. Furthermore, the transient permeate flux is denoted by $J(t)$ and the corresponding steady-state flux is denoted by J^*.

The pseudogel concentration, C_g^*, for a given membrane/solute system can be obtained by extrapolation of the linear part of the curve J^* vs log (C_{FS}). In some systems (see, for example, Ref. 8 for details), $J^* \rightarrow 0$ as $C_{FS} \rightarrow C_g$, where C_g is now called the gel concentration since the permeate flux approaches zero when the feed concentration is equal to C_g. When there is always a residual permeate flow even if $C_{FS} >> C_g^*$, then this residual permeate flux is denoted by J_R^*.

RESULTS

Dead-End Filtration and Modified Fouling Index

The variations of t/V (1/J) with V (Eq. 1) for CTAB in the presence of two electrolytes (NaCl and chromate) as a function of electrolyte concentration are shown in Figs. 3 and 4. It can be seen from these figures that t/V decays initially with increasing V. A further increase in V causes t/V

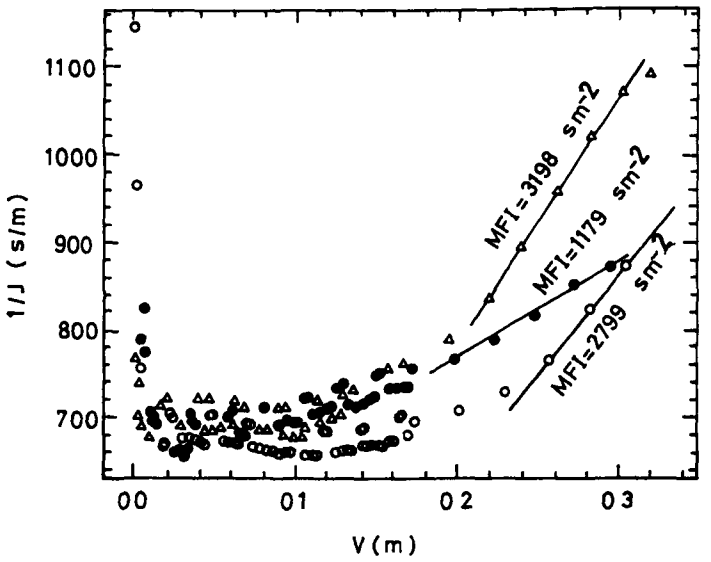

FIG. 3 The effect of NaCl on the evolution of the secondary membrane resistance during the dead-end filtration of CTAB. Modified fouling index is obtained from the slopes of the linear parts of the curves at large permeate volumes, V. ΔP = 150 kPa, T = 30°C, C_{SF} = 4.5 mM. (●) No electrolyte; (○) [NaCl] = 5 mM; (△) [NaCl] = 20 mM.

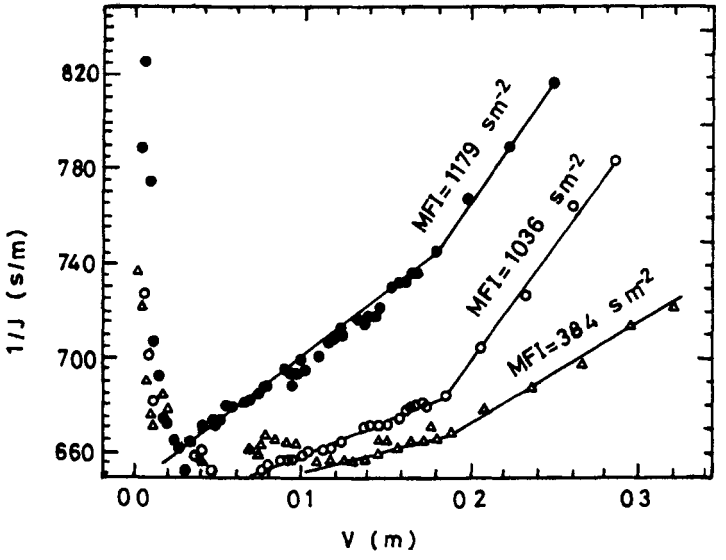

FIG. 4 The effect of chromate concentration on the evolution of the secondary membrane resistance during the dead-end filtration of CTAB. Modified fouling index is obtained from the slopes of the linear parts of the curves at large permeate volumes, V. ΔP = 150 kPa, T = 30°C, C_{SF} = 4.5 mM. (●) $[CrO_4^{2-}]$ = 0; (○) $[CrO_4^{2-}]$ = 0.2 mM; (△) $[CrO_4^{2-}]$ = 0.4 mM.

to increase linearly provided that V is very large. The modified fouling index (MFI) is calculated from the slopes of t/V vs V in the linear region. MFI appear to increase with increasing NaCl concentration (Fig. 3) while the opposite is true for CrO_4^{2-} as shown in Fig. 4. In Fig. 5 the variation of MFI with NaCl or chromate concentrations is illustrated; it indicates a rapid decay of MFI with chromate concentration.

The shape of the curves t/V vs V for surfactant solutions differs from that obtained for the filtration of solid particles. This difference is a result of the conditioning of the membrane surface by the surfactant which results in a decrease of membrane/water interfacial tension and, consequently, the permeate flux increases. As the monolayer surfactant coverage of the membrane gives way to large-scale surfactant deposition which eventually leads to the formation of the secondary membrane, permeate flux starts decreasing. Therefore the cake resistance should be estimated after the formation of the secondary membrane. These observations are in line with the mechanism of crossflow filtration of surfactant dispersions published recently (8–10) which indicate that if the surfactant has a signifi-

cantly higher solubility parameter than the membrane, the permeate flux increases initially (8).

Crossflow Microfiltration

The interaction between the membranes and solute (chromate, CrO_4^{2-}) was investigated initially by feeding a 50-ppm chromate solution containing no surfactant through the filter unit and measuring the chromate rejection. The results indicated no chromate rejection under the prevailing process conditions. A repeat test demonstrated that the experiments were repeatable within $\pm 2\%$.

Development of Chromate and CTAB Rejections

The effect of varying CTAB/chromate concentration ratios (all concentrations are in mM) on the CTAB and chromate rejections was investigated using two different sets of experiments. In the first set of experiments, different CTAB/chromate concentration ratio feed solutions were prepared by maintaining the feed chromate concentration C_{CF} constant while

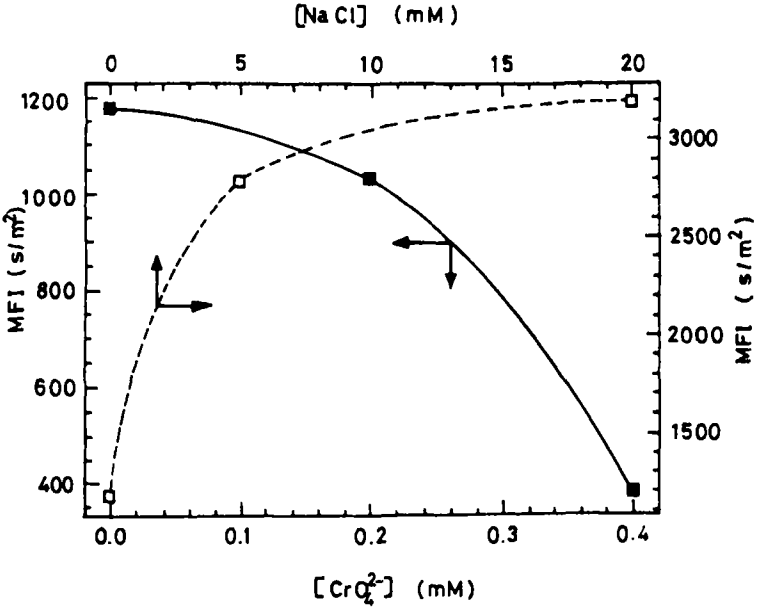

FIG. 5 The variation of modified fouling index, MFI, with chromate or NaCl concentration when the feed surfactant (CTAB) concentration is kept at C_{SF} = 4.5 mM.

changing the CTAB concentration. The CTAB and chromate rejections are shown in Figs. 6 and 7, respectively. As seen from these figures, the rejections of CTAB and chromate increase with increasing CTAB/chromate ratio. It has been observed that at all concentration ratios of CTAB/chromate, the CTAB and chromate rejections curves have similar trends. It can be observed from Figs. 6 and 7 that as the CTAB concentration in the feed increases, the steady-state rejection is established faster.

In the second set of experiments, the CTAB concentration was kept constant at C_{SF} = 4.5 mM [i.e., $C_{SF} = 5x$ (CMC of CTAB)] while changing the chromate concentration. The rejections for chromate and CTAB at different CTAB/chromate ratios are shown in Figs. 8 and 9. As can be seen from these figures, the rejections for CTAB (R_S) and chromate (R_C) increase with increasing CTAB/chromate ratio. Figure 9 illustrates the effect of feed chromate ion concentration (C_{CF}) on the CTAB rejection, R_S.

Steady-State Permeate Flux

The variation of steady-state permeate flux J^* with feed surfactant concentration C_{SF} is shown in Fig. 10 when C_{CF} = 0 or C_{CF} = 0.2 mM. It is possible to obtain the pseudogel concentrations for these two cases by

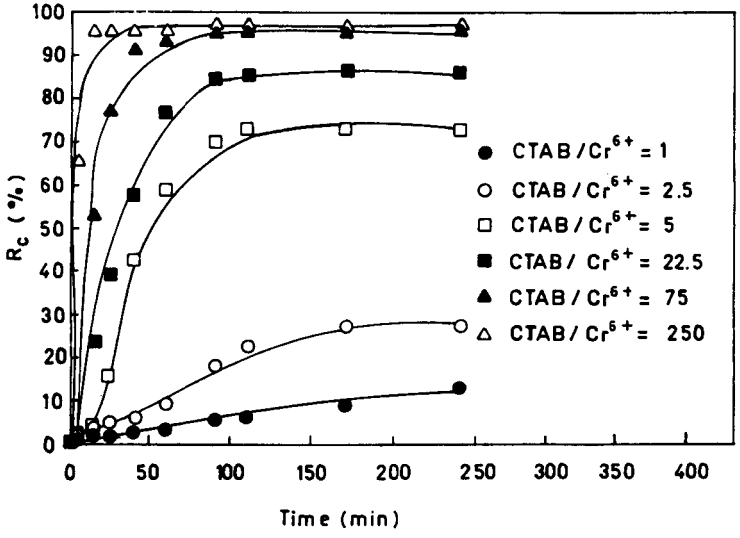

FIG. 6 The variation of transient chromate rejection, R_C, with time as a function of feed CTAB/chromate concentration ratio (C_{SF}/C_{CF}) when the feed chromate concentration is kept at C_{CF} = 0.2 mM, during crossflow filtration.

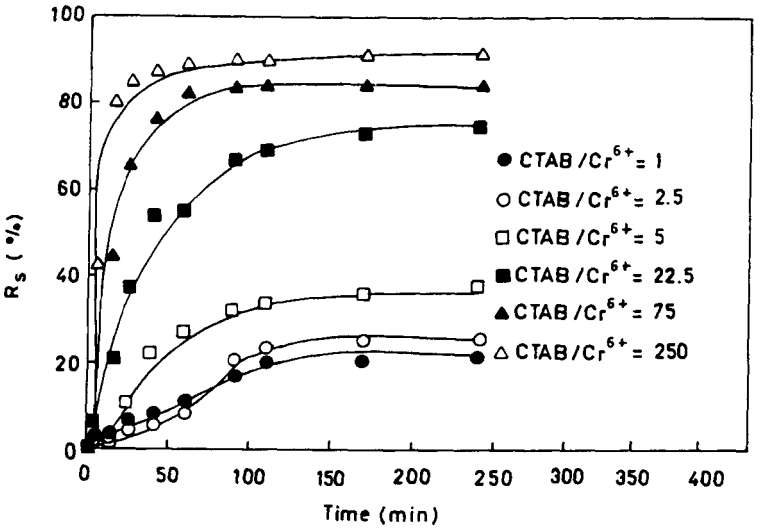

FIG. 7 The variation of transient surfactant (CTAB) rejection, R_S, with time as a function of feed CTAB/chromate concentration ratio (C_{SF}/C_{CF}) when the feed chromate concentration is kept at C_{CF} = 0.2 mM during crossflow filtration.

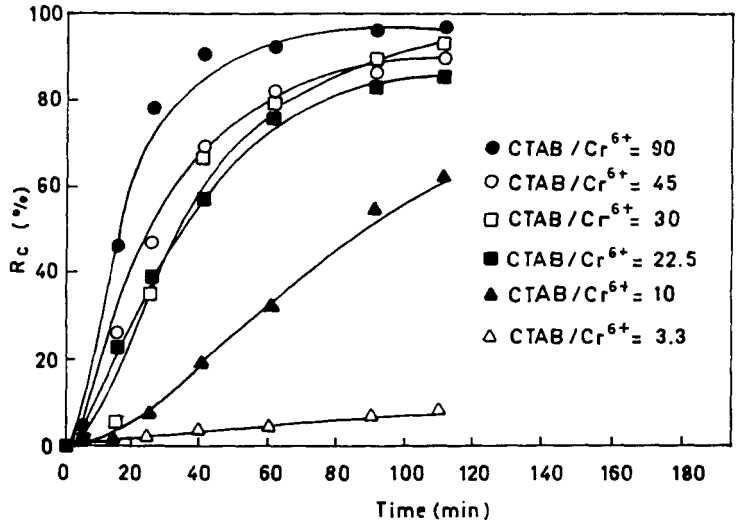

FIG. 8 The variation of transient chromate rejection, R_S, with time as a function of feed CTAB/chromate concentration ratio (C_{SF}/C_{CF}) when the feed CTAB concentration is kept at C_{SF} = 4.5 mM, during crossflow filtration.

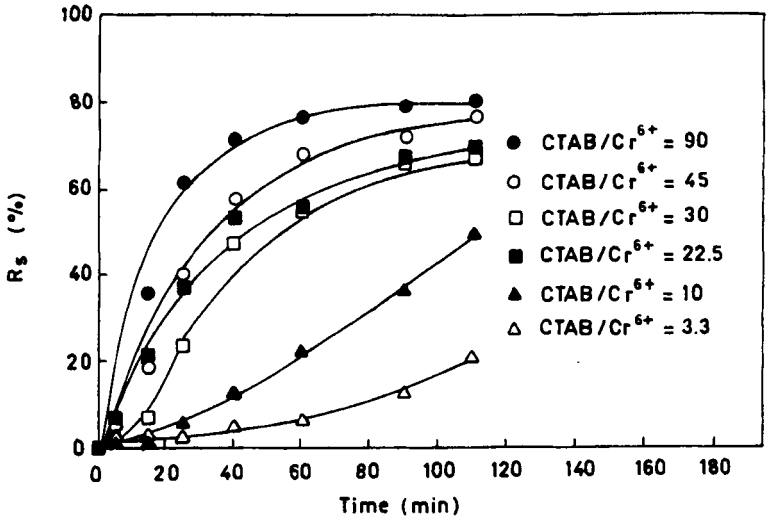

FIG. 9 The variation of transient surfactant (CTAB) rejection, R_S, with time as a function of feed CTAB/chromate concentration ratio (C_{SF}/C_{CF}) when the feed chromate concentration is kept at C_{SF} = 4.5 mM.

extrapolation. When $C_{CF} = 0$, $C_g^* \simeq 66$ mM and when $C_{CF} = 0.2$ mM, $C_g^* \simeq 3.4$ mM. The corresponding residual permeate fluxes are J_R^* ($C_{CF} = 0$) $\simeq$ 150 L/h·m^2 and J_R^* ($C_{CF} = 0.2$ mM) $\simeq$ 500 L/h·m^2. Because C_{CF} is fixed at 0.2 mM, the effect of the chromate is expected to be more significant at low surfactant concentrations. However, Fig. 10 indicates that even at high surfactant concentrations there is a marked difference between the cases when $C_{CF} = 0$ and $C_{CF} = 0.2$ mM, indicating that the chromate ions may be accumulated in the surfactant phase in the secondary membrane.

Steady-State Rejections

Figure 11 illustrates the variation of the steady-state chromate and CTAB rejections, R^*_C and R^*_S, as a function of CTAB/chromate concentration ratio for both sets of experiments. This figure also illustrates the variation of the permeate flux at the same CTAB/chromate concentration ratio for the first set of experiments conducted at constant chromate concentration when $C_{CF} = 0.2$ mM. The steady-state flux J^* for the first set of experiments ($C_{CF} = 0.2$ mM) decreases with increasing CTAB/chromate concentration ratio as indicated in Fig. 11. This is to be expected since, as CTAB/chromate concentration ratio increases, CTAB concentration also increases.

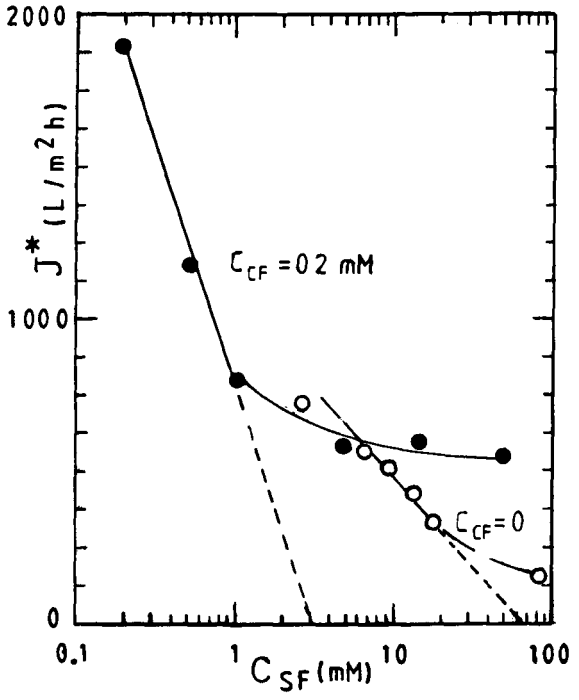

FIG. 10 The variation of the steady-state permeate flux J^* with feed surfactant concentration, C_{SF}, when the feed chromate concentration is C_{CF} = 0 mM (○) or C_{CF} = 0.2 mM (●).

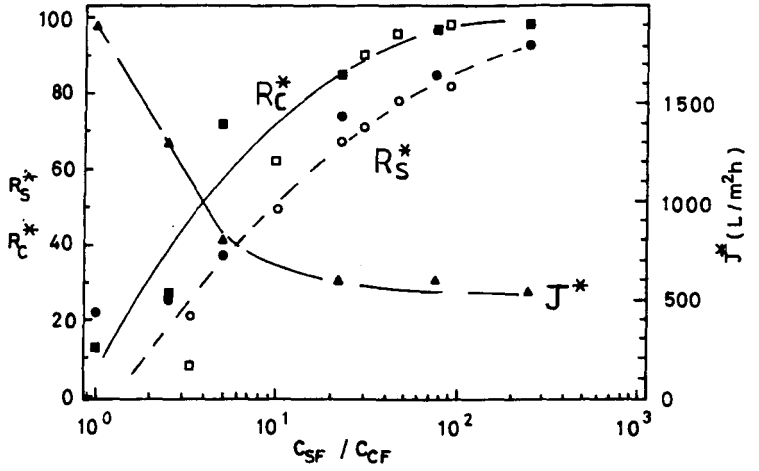

FIG. 11 The variation of the steady-state chromate rejection, R_C^* (■, □) and surfactant (CTAB) rejection, R_S^* (●, ○) as a function of feed CTAB/chromate concentration ratio (C_{SF}/C_{CF}) when either chromate concentration is kept constant at C_{CF} = 0.2 mM (■, ●) or CTAB concentration is kept constant at C_{SF} = 4.5 mM (□, ○). The variation of the steady-state permeate flux, J^*, with C_{SF}/C_{CF} is also shown (▲).

TABLE 1
The Effect of Chromate Concentration on the Permeate Flux
(4.5 mM CTAB for 110 minutes)

Chromate concentration (mM)	0	0.05	0.1	0.15	0.45	0.73
Flux ($L/m^2 \cdot h$)	550[a]	827[a]	839[a]	845[a]	1294[b]	4426[b]

[a] Steady-state flux.
[b] Flux after 110 minutes (steady state not reached).

Table 1 shows the variation of steady-state flux for the second set of experiments (C_{SF} = 4.5 mM) together with the values of flux after 110 minutes of filtration time which was not sufficient to establish steady-state conditions. It can be seen from this table that the increasing chromate concentration causes the steady-state flux to increase. However, the time taken to establish steady state also increases with increasing chromate concentration.

Effects of Feed Composition on Rejections

The effects of feed CTAB and chromate concentrations on the corresponding steady-state permeate CTAB and chromate concentrations, C_S^* and C_C^*, for both sets of experiments are illustrated in Fig. 12 which

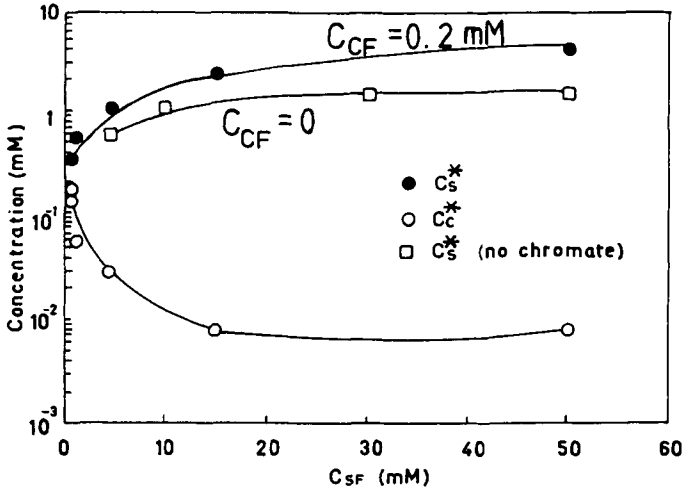

FIG. 12 The variations of the steady-state permeate chromate (C_C^*) and surfactant (C_S^*) concentrations with feed surfactant concentration (C_{SF}) when the feed chromate concentration is kept at C_{CF} = 0.2 mM.

shows that (C_{CF} = 0.2 mM) as the feed CTAB concentration (C_{SF}) increases, chromate concentration in the permeate decreases. However, the decay of chromate concentration in the permeate is very slow when CTAB concentration is greater than ca. 15 mM. Nevertheless, CTAB concentration in the permeate increases (with or without the presence of chromate) with feed CTAB concentration.

When the feed CTAB concentration is kept constant at C_{SF} = 4.5 mM and the feed chromate concentration is increased, both the chromate and CTAB concentrations in the permeate increase as shown in Fig. 13. The increase in the permeate chromate concentration is more significant compared with the increase in the permeate CTAB concentration.

Effect of Chromate Concentration on Modified Fouling Index

The variation of the modified fouling index, MFI, with chromate concentration is shown in Fig. 14. Compared with the MFI values obtained for dead-end filtrations, MFI for crossflow filtration is greater by approximately a factor of two. Nevertheless, MFI decays rapidly to insignificant levels when the chromate concentration is ~1.4 mM. In this case also, CTAB concentration was kept at 4.5 mM.

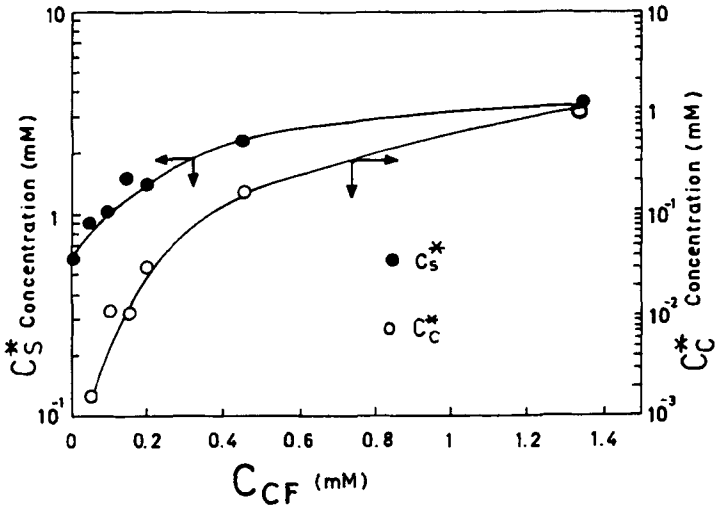

FIG. 13 The variations of the steady-state permeate chromate (C_C^*) and surfactant (C_S^*) concentrations with feed chromate concentration (C_{CF}) when the feed surfactant (CTAB) concentration is kept at C_{SF} = 4.5 mM.

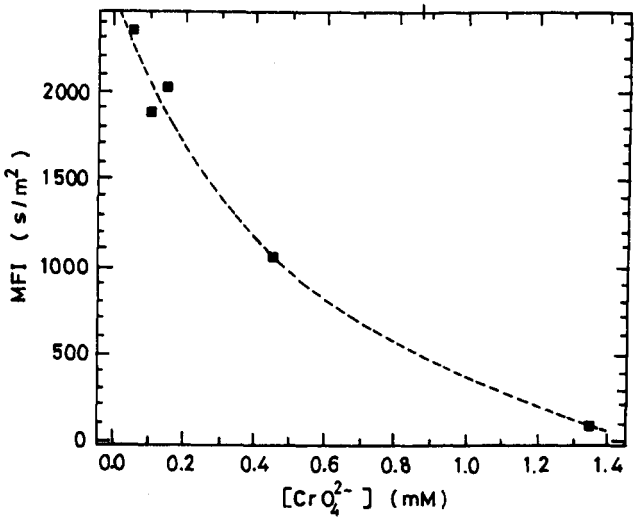

FIG. 14 The effect of chromate concentration on the modified fouling index of CTAB in crossflow microfiltration when feed CTAB concentration is kept at C_{SF} = 4.5 mM.

DISCUSSION

As a result of the formation of a secondary membrane within the pores and on the surface of the primary membrane while the permeate flux decays with time, the surfactant rejection increases provided that wetting of the membrane by water is readily possible (8). The formation of the secondary membrane which, to a large extent, controls the permeate flux and rejection under steady-state conditions, is a result of surfactant deposition on the membrane and subsequent phase change as a result of increased surfactant concentration.

Under steady-state conditions the secondary membrane is in a highly viscous state, such as lamellar or hexagonal phase. The concentration of the surfactant in the secondary membrane can be estimated to a first order from the binary phase diagram of the surfactant/water system.

The binary phase diagram of the CTAB/water system as recently given by Laughlin (20) indicates that, at the temperature of the present study (30°C), the surfactant/water binary system forms an isotropic liquid phase; that is, monomeric surfactant or molecular aggregates of surfactant in water until CMC (~0.9 mM) is reached. After CMC, the isotropic liquid is a micellar dispersion until the surfactant concentration reaches ~240 $g \cdot L^{-1}$ (660 mM) when a transition to a highly viscous hexagonal phase

should take place (20). After the establishment of this phase, we can assume that an overall steady state is established both for permeate flux and surfactant/chromate rejections. It was shown by Akay and Wakeman (9) that there are differences in the structure of the freely grown viscous surfactant phase and that grown during crossflow filtration. These differences are attributed to the presence of permeate flow and surfactant/membrane interactions in the presence of water. The effects of flow field on the microstructure concentration distribution and microstructure morphology are well known in many structured fluids (21–23). In the present study we are concerned with the effects of chromate ions on the establishment of the secondary membrane and its retention and permeate characteristics.

Establishment of the Secondary Membrane

The development of the secondary membrane can be inferred by plotting the time-dependent variation of permeate flux $J(t)$ and the dimensionless permeate concentrations of the surfactant $C_S(t)/C_{SF}$ and chromate $C_C(t)/C_{CF}$. The results are shown in Fig. 15 and 16 for both sets of experiments. Figure 15 refers to the case when C_{CF} = 0.2 mM and CTAB

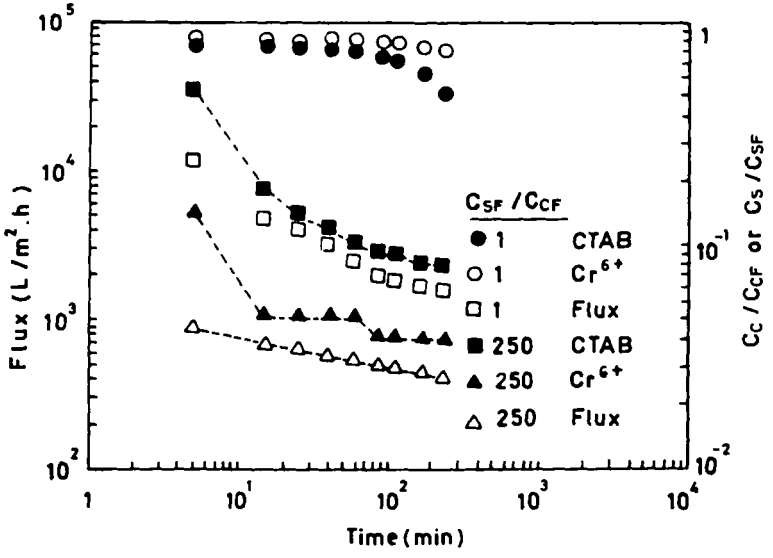

FIG. 15 Transient behavior of permeate flux, J(t), and the dimensionless chromate, C_C(t)/C_{CF}, and surfactant (CTAB) concentration ratio, $C_S(t)/C_{SF}$, at various feed CTAB/chromate concentration ratios, C_{SF}/C_{CF}, when chromate concentration is kept constant at C_{CF} = 0.2 mM.

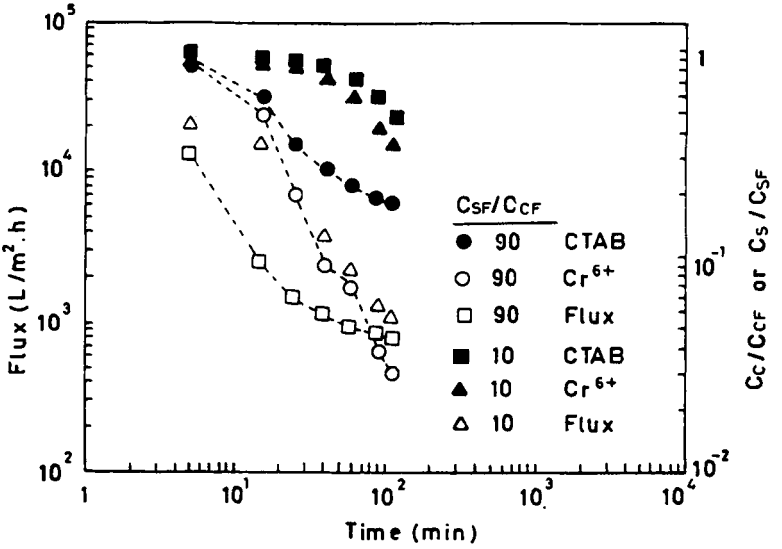

FIG. 16 Transient behavior of permeate flux, $J(t)$, and the dimensionless chromate, $C_C(t)/C_{CF}$, and surfactant (CTAB) concentration ratio, $C_S(t)/C_{SF}$, at various feed CTAB/chromate concentration ratios, C_{SF}/C_{CF}, when CTAB concentration is kept constant at C_{SF} = 4.5 mM.

concentration is changed, while Fig. 16 deals with the case when C_{SF} = 4.5 mM and chromate concentration is changed. A close examination of Fig. 15 shows that when $C_{SF}/C_{CF} = 1$, although the permeate flux $J(t)$ decays rapidly in the first 100 minutes, CTAB and chromate concentrations in the permeate are just below that of the corresponding feed concentrations, i.e., very small rejection. After ~100 minutes of filtration, permeate flux approaches steady state [i.e., $J(t) \rightarrow J^*$] and the decay of the permeate CTAB and chromate concentrations accelerates. However, the experimental time is not sufficient to establish the overall steady-state conditions for the rejections. Due to the low levels of CTAB per chromate ion, we observe that chromate concentration in the permeate decays more slowly compared with CTAB concentration.

When CTAB/chromate concentration ratio is very high (C_{SF}/C_{CF} = 250) at the same chromate concentration (C_{CF} = 0.2 mM), permeate flux decays very rapidly within 4 minutes, reaching a state where it continues to decay very slowly. In this case, both CTAB and chromate permeate concentrations decay very rapidly initially and reach a state where the decay is slow. In this case the decay of chromate is considerably faster than that of CTAB. We can thus conclude that all of the chromate ions

are bound to the micelles and that due to the high CTAB concentration, the secondary membrane is very efficient in retaining both chromate and CTAB.

In Fig. 16 the feed CTAB concentration is kept constant at C_{SF} = 4.5 mM and the C_{SF}/C_{CF} ratio is changed. If the chromate concentration is low (i.e., C_{SF}/C_{CF} = 90), flux decays faster compared with the case when the chromate concentration is high (C_{SF}/C_{CF} = 10). However, the steady-state fluxes appear to be similar. The decay of the permeate surfactant and chromate concentrations shows the reverse trend. When C_{SF}/C_{CF} = 10, dimensionless permeate CTAB and chromate concentrations (C_S/C_{SF} and C_C/C_{CF}) are higher than the case when C_{SF}/C_{CF} = 90. In both cases, however, $C_S/C_{SF} > C_C/C_{CF}$. Once again, at high feed surfactant concentrations (C_{SF}/C_{CF} = 90) the decay of the surfactant starts after some 5 minutes, while at low CTAB concentrations (C_{SF}/C_{CF} = 10) the corresponding decay starts after about 40 minutes.

The above discussion indicates that the mechanism of the secondary membrane formation is in agreement with that given by Akay and Wakeman (9). The effect of the chromate ions is to delay the formation of the secondary membrane which results in higher permeate flux but low surfactant and chromate rejections. The reduction of the secondary membrane resistance in the presence of CrO_4^{2-} has recently been confirmed using pulsed proton relaxation NMR (24).

Steady-State Characteristics of the Separation Process and Secondary Membrane Structure

Under steady-state conditions, high chromate concentration appear to reduce the rejection of both chromate and surfactant which can be observed from Figs. 12 and 13 and from the discussion above based on Figs. 15 and 16. These results indicate that in the presence of chromate ions, the secondary membrane is more porous compared with the secondary membrane without metal ions as also confirmed independently (24). Therefore, we should expect that the modified fouling index MFI in the presence of chromate ions will decrease with increasing chromate concentration. This is in fact what is observed both in dead-end filtration (Figs. 3 and 5) and crossflow filtration (Fig. 14). However, the effect of NaCl addition, albeit at higher loadings, is to increase the fouling index as shown in Figs. 4 and 5. The decrease of permeate flux due to the addition of NaCl has been observed previously (6, 14).

The effect of electrolyte addition to the surfactant/water binary system should be explained, in part, by the modification of the surfactant electrical double layers by salt. The addition of NaCl results in the breakdown

of viscous surfactant phases (such as hexagonal phase) to form the micellar phase, thus effectively increasing the surfactant concentration necessary to form the secondary membrane. This increase in the surfactant concentration results in a more dense secondary membrane structure, thus increases the fouling index. As the NaCl concentration is increased above 100 mM, liquid crystalline phases form (25). It is possible, due to the high valency and large size of the chromate ions, to form liquid crystalline structures at low surfactant concentrations (25), hence the increases in porosity of the secondary membrane and permeate flux.

In the above discussion we did not consider the effect of osmotic pressure on rejection. The effect of osmotic pressure resulting from the high concentration gradient across the membrane is to reduce the effective transmembrane pressure drop, and therefore a reduction in the permeate flux should be expected (5). As seen from the present results, osmotic pressure due to chromate ions can be ignored since their presence increases the permeate flux and their concentration is low compared with that of the surfactant.

CONCLUSIONS

Removal of chromate ions from water using a cationic surfactant, cetyl trimethylammonium bromide, CTAB, by crossflow microfiltration was investigated. The main emphasis of the investigations was to evaluate the effects of surfactant and chromate concentrations on the transient and steady-state behavior of permeate flux and chromate and surfactant rejections. It was found that the presence of chromate ions delayed the time taken to establish the steady-state conditions for permeate and surfactant and chromate rejections. High chromate/CTAB concentration ratios also resulted in the lowering of the rejections, but there was an increase in the residual permeate flux J_R^* when the feed surfactant concentration was above the pseudogel concentration C_g^*.

These results can be explained by considering the dynamics of the secondary membrane formation during crossflow filtration. The model given by Akay and Wakeman (9) is applicable to the present system except that one needs to take into account the modification of the surfactant electrical double layers by the addition of electrolytes. Reduction of the hydrodynamic resistance of the secondary membrane in the presence of chromate is a result of the formation of a low viscosity, high-water content liquid crystalline phase which we may assume to be a hexagonal phase. The reduction in the resistance of the secondary membrane was independently confirmed by dead-end filtration experiments in which the fouling index of the surfactant filtration layer was measured. The result indicated reduction of the fouling index with increasing chromate concentration. How-

ever, the effect of addition of NaCl was to increase the fouling index, in confirmation with the effects observed in crossflow microfiltration (7, 14) or ultrafiltration (7). It is therefore clear that the electronic structure and size of the ions can have entirely different effects on the permeate and rejection characteristics of the secondary membranes during the filtration of surfactant dispersions in the presence of electrolytes.

NOTATION

C_C, C_S	transient chromate and surfactant concentrations in the permeate
C_C^*, C_S^*	steady-state chromate and surfactant concentrations in the permeate
C_{CF}, C_{SF}	chromate and surfactant concentrations in the feed
C_g, C_g^*	gel and pseudogel concentrations (surfactant)
CMC	critical micellar concentration
J, J^*	transient and steady-state permeate fluxes
J_R^*	residual permeate flux when $C_{SF} > C_g^*$
MFI	modified fouling index
R_C, R_C^*	transient and steady-state chromate rejections
R_m	membrane resistance
R_S, R_S^*	transient and steady-state surfactant rejections
t	time
V	volume of permeate per unit filtration area
α	specific cake resistance
ΔP	transmembrane pressure drop
μ	viscosity of permeate

REFERENCES

1. S. D. Christian, S. N. Bhat, and E. E. Tucker, "Micellar Enhanced Ultrafiltration of Chromate Anion from Aqueous Streams," *AIChE J.*, *34*, 189–194 (1988).
2. J. F. Scamehorn and J. H. Harwell (Eds.), *Surfactant Based Separation Processes*, (Surfactant Science Series, Vol. 33), Dekker, New York, NY, 1989.
3. G. Morel, A. Graciaa, and J. Lachaise, "Enhanced Nitrate Ultrafiltration by Cationic Surfactant," *J. Membr. Sci.*, *56*, 1–12 (1991).
4. J. F. Scamehorn, S. D. Christian, D. A. El-Sayed, and H. Uchiyama, "Removal of Divalent Metal Cations and Their Mixtures from Aqueous Streams Using Micellar Enhanced Ultrafiltration," *Sep. Sci. Technol.*, *29*, 809–830 (1994).
5. J. H. Markels, L. Scott, and C. J. Radke, "Cross-Flow Ultrafiltration of Micellar Surfactant Solutions," *AIChE J.*, *41*, 2058–2066 (1995).
6. D. Bhattacharyya, A. B. Jumawan, R. B. Grieves, and L. R. Harris, "Ultrafiltration Characteristics of Oil–Detergent–Water Systems: Membrane Fouling Mechanisms," *Sep. Sci. Technol.*, *14*, 529–549 (1979).
7. G. Akay and R. J. Wakeman, "Ultrafiltration and Microfiltration of Surfactant Disper-

sions—An Evaluation of Published Research," *Chem. Eng. Res. Des.*, *71*, 411–420 (1993).
8. G. Akay and R. J. Wakeman, "Crossflow Microfiltration Behaviour of a Double Chain Cationic Surfactant Dispersion in Water. I. Effect of Process and Membrane Characteristics on Permeate Flux and Surfactant Rejection," *Chem. Eng. Sci.*, *49*, 271–283 (1994).
9. G. Akay and R. J. Wakeman, "Mechanisms of Permeate Flux Decay, Solute Rejection and Concentration Polarisation in Crossflow Filtration of a Double Chain Ionic Surfactant Dispersion," *J. Membr. Sci.*, *88*, 177–195 (1994).
10. G. Akay and R. J. Wakeman, "Permeate Flux Decay during Crossflow Microfiltration of a Cationic Surfactant Dispersion," *Filtr. Sep.*, *31*, 727–731 (1994).
11. R. J. Wakeman and G. Akay, "Flux Decay and Rejection during Micro- and Ultra-Filtration of Hydrophobically Modified Water-Soluble Polymers," *J. Membr. Sci.*, *91*, 145–152 (1994).
12. G. Akay, Z. Bhumgara, and R. J. Wakeman, "Self-Supported Porous Channel Membrane Modules: Preparation, Properties and Performance," *Chem. Eng. Res. Des.*, *73*, 783–796 (1995).
13. R. J. Wakeman and G. Akay, "Concentration and Fractionation of Polyvinyl Alcohol-Anionic Surfactant Stabilised Latex Dispersions by Microfiltration," *J. Membr. Sci.*, *106*, 57–65 (1995).
14. G. Akay and R. J. Wakeman, "Electric Field Intensification of Surfactant Mediated Separation Processes," *Chem. Eng. Res. Des.*, *74*, 517–525 (1996).
15. G. Akay and R. J. Wakeman, "Electric Field Enhanced Crossflow Microfiltration of Hydrophobically Modified Water Soluble Polymers, *J. Membr. Sci.*, In Press.
16. G. Akay, A. Cakici, B. Keskinler, and R. J. Wakeman, In Preparation.
17. E. Yildiz, B. Keskinler, T. Pekdemir, A. Cakici, and G. Akay, "Surfactant Enhanced Crossflow Filtration in Nitrate Removal from Water," in *Science, Engineering and Technology of Intensive Processing*, (G. Akay and B. J. Azzopardi, Eds.), University of Nottingham, Nottingham, 1995, pp. 121–124.
18. E. Yildiz, T. Pakdemir, B. Keskinler, A. Cakici, and G. Akay, "Surfactant-Mediated Separation Processes: Surfactant-Enhanced Crossflow Filtration in Nitrate Removal from Water," *Chem. Eng. Res. Des.*, *74*, 546–553 (1996).
19. R. Rautenbach and R. Albrecht, *Membrane Processes*, Wiley, New York, NY, 1984.
20. R. G. Laughlin, "Aqueous Phase Science of Cationic Surfactant Salts," in *Cationic Surfactants* (Surfactant Science Series, No. 37) (D. N. Rubingh and P. M. Holland, Eds.), Dekker, New York, NY, 1991.
21. G. Akay, in *Encyclopedia of Fluid Mechanics*, *Vol. 1* (N. P. Cheremisinoff, Ed.), Gulf Publishing, Houston, TX, 1986, Chap. 35, pp. 1155–1204.
22. G. Akay, "Flow Induced Phase Inversion Agglomeration: Fundamentals and Batch Processing," *Polym. Eng. Sci.*, *34*, 865–880 (1994).
23. G. Akay, "Flow Induced Phase Inversion in Powder Structuring by Polymers," in *Polymer Powder Technology* (M. Narkis and N. Rosenzweig, Eds.), Wiley, New York, NY, 1995, Chap. 20, pp. 542–587.
24. A. Kazeem, G. Akay, W. Derbyshire, and P. P. Morales, *Effect of Heavy Metal Ions on Surfactant Phase Behaviour*, Presented at IChemE Research Event, 7–9 April 1997, University of Nottingham, Nottingham, UK, pp. 619–622.
25. K. Fontell, *Colloidal Dispersions and Micellar Behavior*, ACS Symp. Ser. 9, 1975, p. 270.

Received by editor July 31, 1996
Revision received December 1996